Cluster model of baryons

K. F. Liu
Department of Physics and Astronomy, University of Kentucky, Lexington, Kentucky 40506

C. W. Wong
Department of Physics, University of California, Los Angeles, California 90024
(Received 7 January 1983)

Baryons are studied in the constituent quark model by reducing the three-body problem to equivalent two-body problems involving a diquark and a quark. Rotational and radial excitations of the diquark or of the third quark are calculated by using nonrelativistic mesonic $q\bar{q}$ potentials which are fitted to meson masses. The results are found to be in good agreement with experimental baryon masses. A strong suppression of the mesonic spin-orbit potential is required for light baryons, in agreement with the conclusion of other authors.

I. INTRODUCTION

Nonrelativistic (NR) potential models of quark dynamics have been used for quite some time now for the description of baryons.[1–7] The masses of interest are made up partially of kinetic energies and partially of potential energies. It is obvious that a NR potential model does not describe correctly the kinetic energies of light relativistic quarks.

The situation does not appear so hopeless if one concentrates instead on the total excitation energies, using a NR potential which is already fitted, say, to be masses of $q\bar{q}$ mesons. Such a model is essentially a procedure for mass extrapolation which is more inclusive than those based on algebraic mass formulas. It has the further advantage of being applicable to complicated multiquark systems, if we could isolate model-independent from model-dependent features.[8] Other more specific arguments for the possible usefulness of the NR quark model for light hadrons involve magnetic moments[1,9] and hadronic decays of baryons.[4,5]

In the simplest color-dependent potential model, the quark-quark potential in baryons is exactly half of the quark-antiquark potential in mesons. This assumption appears to work reasonably well at the level of mass formulas[10,11] or of simple potential model.[12,13] This suggests that many features of quark dynamics can be described satisfactorily in terms of pairwise interactions only, i.e., that many-body forces do not have to be mentioned explicitly, even if they might be important in other aspects of quark dynamics.

Indeed, notable successes have been obtained by Isgur and Karl[4–7] using a one-gluon-exchange interaction in the Breit-Fermi form. They found that the mass splitting of baryons and their mixing angles in the SU(6) classification are well described by the spin-spin and tensor parts of the Breit-Fermi interaction. However, the spin-orbit potential has to be strongly suppressed.

We have shown in an earlier paper[11] that the parameters used to fit baryon (ground-state) masses in the mass formula of De Rújula, Georgi, and Glashow[10] can also be used to describe meson masses if a size correction is included. It therefore appears profitable to study the phenomenology of baryonic excitations using potentials fitted to meson masses. Furthermore, if the three-body problem is treated by a cluster model[14] to be described in Sec. II, the problem reduces to equivalent two-body problems involving either diquark excitations or quark-diquark excitations, or both. In this way, the similarities and differences between baryonic and mesonic systems can be made even clearer and arbitrary rotational and radial excitations can be calculated.

This cluster model can be used with any potential model, relativistic as well as NR. For definiteness we use the NR meson potential of Liu and Wong.[15] The relativistic quark-diquark cluster model has been studied by Lichtenberg and collaborators.[16] The properties of the resulting diquark clusters are described in Sec. II. Section III gives a brief summary of the calculated results for ground state baryon masses. The general characters of the rotational and radial excitations in the Λ and Σ families of baryons are described in Sec. IV. More detailed descriptions of the results for the lowest negative- and positive-parity excitations, including N^* and Δ^* baryons, are given in Secs. V and VI, respectively. Section VII contains brief concluding remarks.

II. A CLUSTER MODEL FOR HADRONIC EXCITED STATES

The cluster model described below is designed for the study of the excitations of one internal degree of freedom. In this way, states belonging to the same Regge trajectory can be isolated from the many excited states of the system. The model is constructed as follows: (1) One of the internal coordinates is selected as the rotational coordinate under discussion. (2) The remaining internal coordinates are treated with the help of variational wave functions. Simple Gaussian wave functions are used in the calculations reported here. (3) An effective potential in the chosen rotational coordinate is constructed after integrating over the variational wave functions for the other internal coordinates (to be called variational coordinates below). This potential includes spectator contributions from the variational coordinates. We make one exception in this scheme in order to simplify the calculation. All cluster calculations are performed in the single-channel approximation. Any configuration mixing is treated by first-order perturbations, as will be described later. (4) The resulting Schrödinger equation in the rotational coor-

dinate is solved for different angular momenta to generate a Regge trajectory. The equation can also be solved for radial excitations. We show only a few such solutions since only a few radially excited states are known experimentally. (5) The variational parameter is separately varied to minimize the energy of each rotational state. In this way, the effects of centrifugal stretching can be included.

For q^3 baryons, there are two internal coordinates,

$$\vec{\rho}=\vec{r}_1-\vec{r}_2, \text{ and } \vec{\lambda}=\vec{R}_{12}-\vec{r}_3 , \tag{1}$$

where

$$\vec{R}_{12}=(\vec{r}_1+\vec{r}_2)/2 .$$

The resulting excitations will be called the ρ mode and the λ mode, respectively. The quarks 1 and 2 make up what we shall call the diquark part of the baryon. Antisymmetrization of the wave function is simplified by putting quarks of the same flavor in the diquark whenever possible.

The color operator in the diquark has the matrix element

$$\langle\lambda_1\cdot\lambda_2\rangle_\alpha=\begin{cases}-\frac{8}{3} & \text{in } \alpha=(3\times3)\bar{3} ,\\ \frac{4}{3} & \text{in } \alpha=(3\times3)6 ,\end{cases} \tag{2}$$

as compared to the matrix element of $-\frac{16}{3}$ in the mesonic $(3\times\bar{3})1$ state. This means that the two quarks are confined to each other in the color representation $\bar{3}$, but tend to keep away from each other in representation 6. Color-6 components do not appear in q^3 baryons, but can appear in multiquark systems.

Thus only the color-$\bar{3}$ component forms a relatively well-defined diquark structure in hadrons. Its mass in our model may be written as

$$M(q^2)=m_1+m_2+\langle p^2\rangle/2\mu + \tfrac{1}{2}\left\langle kr+b-\tfrac{4}{3}\alpha_s\left[\frac{1}{r}+\frac{1}{m_1m_2}f_{\rm BF}(r)\right]\right\rangle , \tag{3}$$

where m_i are quark masses and μ is the reduced mass. The last term is just half of a $q\bar{q}$ meson potential,[15] and contains a modified Breit-Fermi part of the form

$$f_{\rm BF}(r)=S(r)\vec{S}_1\cdot\vec{S}_2+W(r)\vec{L}\cdot\vec{S}+V_T(r)S_T , \tag{4}$$

where

$$S(r)=-\frac{2}{3}\left\{\frac{4}{\pi^{1/2}r_0{}^3}\exp\left[-\left(\frac{r}{r_0}\right)^2\right]\right\} ,$$

$$W(r)=-\frac{3}{2}\left\{1-\exp\left[-\left(\frac{r}{a_0}\right)^2\right]\right\}\Big/r^3 ,$$

$$V_T(r)=-\frac{1}{4}\left\{1-\exp\left[-\left(\frac{r}{a_0}\right)^2\right]\right\}\Big/r^3 , \tag{5}$$

$$S_T=3\vec{\sigma}_1\cdot\hat{r}\vec{\sigma}_2\cdot\hat{r}-\vec{\sigma}_1\cdot\vec{\sigma}_2 ,$$

$$r_0=a_0/2.7 .$$

The additive constant b is taken to be -82 MeV. The other potential parameters, fitted separately to different families of mesons,[15] are shown in Table I. The quark masses used are 0.12 (0.334, 1.51, 4.83) GeV for the flavor u or d (s,c,b). The u,d quark mass has been chosen to fit the proton size rather than its magnetic moment.

Table II gives the $1s$ diquark masses and rms radii calculated variationally with Gaussian wave functions. We see that diquark masses are roughly the same as mesonic masses, except that the spin-spin splittings are only a fifth as strong. Diquark sizes are about a third bigger than meson sizes, so that diquarks should probably not be considered a structurally independent part of hadrons, except in those special situations where they are clearly separated from the rest of the hadron.

III. GROUND-STATE BARYONS

We first test the cluster model on the SU(6) 56-plet baryon ground states. The nucleon mass calculated with the same variational Gaussian function between all quark pairs is 1065 MeV. This decreases to 1060 MeV if the Gaussian falloff constants in the ρ and λ modes are varied independently. An even better result of 1051 MeV is obtained by treating the λ wave functions by means of a radial Schrödinger equation. We shall refer to this as the result of our cluster model. It is actually possible to improve the ρ wave function also. This has been done by Rondinone[12] using an earlier version of our potential. Our approximate result is quite adequate for the present purpose of studying baryonic excitations. It shows in particular that Gaussian variational wave functions give fairly good results.

The mass calculated in the same way for Δ is 1338 MeV. Then the calculated Δ-N mass splitting is in good agreement with experiment, but the absolute masses are too high by about 110 MeV. To compensate for this, we simply assume that the additive constant b in Eq. (3) for q^2 pairs should be taken to be

TABLE I. Parameters of the Liu-Wong potential. The parameters are determined through the following formulas:

$$\alpha_s(V)=1.4/[1+1.295\ln(r_\rho/r_V)] ,$$

where r_V is the rms radius of the vector meson V in each family; $k=[\mu\omega^3(V)/4]^{1/2}$, where

$$\omega(V)=\{0.75/[1+0.4313\ln(r_\rho/r_V)]\} \text{ GeV} ;$$

$$r_0(V)=1.05(r_V/r_\rho)^{2.06} \text{ fm} ,$$

and $a_0=2.7r_0$.

Family	m_Q (GeV)	α_s	k (GeV^2)	a_0 (fm)
ρ/ω	0.12	1.4	0.0795	2.84
ϕ	0.334	0.88	0.101	1.10
ψ/J	1.51	0.54	0.1492	0.224
Υ	4.83	0.40	0.205	0.056
K^*		1.14	0.0864	1.97
D^*		1.00	0.090	1.50
F^*		0.73	0.113	0.65
D_b^*		0.97	0.090	1.39
F_b^*		0.69	0.116	0.54

TABLE II. Comparison of calculated diquark properties with the calculated properties of the meson of the same flavor and spin. ($q=u$ or d.)

		Diquark			Meson	
Flavor	S	M (GeV)	$\langle r^2\rangle^{1/2}$ (fm)	$\alpha'/\alpha'(q^2)$	M (GeV)	$\langle r^2\rangle^{1/2}$ (fm)
qq	0	0.50	0.73	1.0	0.24	0.53
	1	0.65	0.93		0.77	0.72
ss	1	1.02	0.56	1.4	1.02	0.45
cc	1	3.19	0.29	2.3	3.10	0.21
bb	1	9.72	0.16	3.3	9.46	0.11
qs	0	0.73	0.66		0.55	0.46
	1	0.82	0.78	1.2	0.90	0.60
qc	0	1.94	0.66		1.90	0.48
	1	1.96	0.70	1.3	2.01	0.52
qb	0	5.26	0.67		5.26	0.49
	1	5.27	0.68	1.3	5.30	0.51

$$b=-157\ \text{MeV}\ . \tag{6}$$

With this adjustment the calculated masses are found in Table III to be within about 25 MeV of experimental masses. This is about the same in quality as the fit to experimental meson masses used originally to define the potential parameters.[15] We therefore conclude that at this level of accuracy mesonic potentials can indeed be used for the study of baryonic systems. This conclusion is in agreement with those of other authors.[12,13]

IV. EXCITED BARYONS IN THE ρ AND λ MODES

We now turn our attention to our main concern of baryonic excitations.

Rotational excitations within a diquark (i.e., ρ mode) are expected to give Regge trajectories which are roughly linear in Chew-Frautschi plots. However, their Regge slopes α' are not expected to be identical to those of the corresponding meson, because α' is inversely proportional to the square of the characteristic energy scale of the problem:

$$\omega^{-2}=(\mu/k_{\text{eff}}{}^2)^{2/3}\ , \tag{7}$$

where

$$k_{\text{eff}}=-\tfrac{3}{16}\langle\lambda_1\cdot\lambda_2\rangle_{\bar{3}}k$$

is the strength of the linear confinement potential. Since $\langle\lambda_1\cdot\lambda_2\rangle$ for color-$\bar{3}$ diquarks is only half of the mesonic value, its Regge slope is larger by a factor of $2^{4/3}\cong 2.5$. The calculated result for q^2 ($q=u,d$) diquarks is about 2.8 GeV^{-2} in agreement with this expectation.

In our model, the Regge slope is effectively flavor dependent. The expected Regge slope expressed in terms of the Regge slope $\alpha'(q^2)$ of light ($q=u,d$) diquarks is given in the fifth column of Table II. We see that they do not differ greatly from 1 except for the c^2 and b^2 diquarks.

Rotational excitations in the ρ mode are excitations of the diquark. Its Regge slopes are not those of isolated diquarks however, because the third, or spectator, quark also contributes.

The Hamiltonian for the ρ mode takes the following form in the cluster model:

$$\begin{aligned}H_\rho=&m_1+m_2+m_3+\langle P_\lambda{}^2/2\mu_3\rangle_{L=0}+P_\rho{}^2/2\mu_{12}+\lambda_1\cdot\lambda_2V_{12}\\&+(\lambda_1+\lambda_2)\cdot\lambda_3\{C[V_{13}^C](\rho/2)+2\vec{S}_{12}\cdot\vec{S}_3C[V_{13}^{SS}](\rho/2)+(\tfrac{1}{2}\vec{S}_{12}+\vec{S}_3)\cdot C[\vec{L}_{13}V_{13}^{SO}](\rho/2)\\&+2(3\vec{S}_{12}\cdot\hat{\rho}\,\vec{S}_3\cdot\hat{\rho}-\vec{S}_{12}\cdot\vec{S}_3)C[V_{13}^T](\rho/2)\}\ ,\end{aligned} \tag{8}$$

where $\langle P_\lambda{}^2/2\mu_3\rangle_{L=0}$ is the expectation value of the kinetic energy of the third quark in a ground-state λ mode, C is a convolution operator which gives the folded spectator contribution. The precise forms of C are given in the Appendix. At large ρ, both quarks in the diquark are far from the spectator. The spectator contribution then comes primarily from the long-range confinement potential. At large ρ, the spectator quark is roughly midway between those in the diquark, i.e., $r_{13}\cong r_{12}/2$, the convolution $C[V_{13}^C]$ then simplifies to just $V_{12}^C/2$ if the confinement potential is linear. This means that the spectator contributes the same amount as the diquark itself, namely, half of the corresponding mesonic value. As a result, the spectrum for large orbital excitations is identical to the corresponding mesonic spectrum.

At small ρ, the spin-spin terms are also important. However, the spectator contributions from this spin-spin

TABLE III. Masses (in MeV) of ground-state baryons. The nucleon mass has been used to determine the overall additive constant of Eq. (6).

	Calculated	Experimental
N	(939)	939
Λ	1088	1116
Σ	1184	1193
Ξ	1312	1318
Δ	1226	1232
Σ^*	1350	1385
Ξ^*	1502	1533
Ω	1619	1672
Λ_c	2222	2282
Σ_c	2404	2450?
Λ_b	5518	5500?
Σ_b	5737	

potential vanish for spin-singlet diquarks. Consequently, the total color-magnetic (CM) interaction is only half as attractive as that in the corresponding mesons, so that the calculated excitation energies

$$\Delta E_L = E_L - E_0 \tag{9}$$

for baryons are smaller than those calculated for mesons for low orbital excitations.

This situation is illustrated in Table IV which compares the calculated excitation energies of Λ hyperonic states with those calculated for nonstrange spin-singlet mesons.[15] (The latter are not the actual experimental results, since the potential model does not distinguish between π and η, reproducing only the isospin-averaged meson masses.)

An additional effect appears in baryons due to the decrease in kinetic energy of the spectator in response to the centrifugal stretching of the diquark on orbital excitations. This is quite significant in ΔE_1, where it accounts for about 0.06 GeV of the 0.2-GeV difference between the Λ and the mesonic results.

For spin-triplet diquarks, the spectator contribution from the spin-spin potential is attractive. It is stronger than but differs in sign from, the repulsive diquark contribution. The resulting cancellation makes the total CM interaction much less important. However, the centrifugal stretching effect in the spectator kinetic energy is still present. For example, it accounts for 0.10 (0.12) GeV of the difference in ΔE_1 (ΔE_2) shown in Table IV between the Σ hyperonic states and the spin-triplet nonstrange mesonic states. Except for this correction, the excitation energies of Σ are similar to those in spin-triplet mesons even at low orbital excitations.

Similar results can be obtained for the Λ_i and Σ_i families in which the third or strange quark in Λ or Σ is replaced by a heavy quark Q_i. We find, in Table V, that the excitation energies ΔE_L are basically independent of the flavor of Q_i, in spite of the fact that the effective interaction has flavor-dependent parameters. The reason is that the meson spectra to which the interaction parameters are fitted are basically flavor independent. Table V shows that some flavor dependence does appear in radial excitation.

We turn next to excitations in the λ mode, i.e., excitations of the third quark against the diquark cluster in its ground state. The Hamiltonian is similar to that shown in Eq. (8) except that (1) the $L=0$ expectation value is taken for the diquark kinetic and potential energies and (2) the convolution operator involves an average over the diquark wave function. The details are given in the Appendix. One simplifying feature is that the confinement potential for large λ has the mesonic value. However, the diquark mass is greater than the single quark mass, so that the excitation energies, as characterized by the ω parameter of Eq. (7), is decreased. We do not use the diquark mass of Table II, but treat it variationally in each calculation. This tends to increase it, leading to a reduced energy scale ω.

This effect can be seen by comparing the calculated excitation energies shown in Table VI with the corresponding mesonic results. For example, the Λ and Σ excitation energies of the first column should be compared with those of K and K^* mesons, respectively, namely, $\Delta E_L = 0.73$ (1.14) GeV for $L=1(2)$ for spin-singlet states

TABLE IV. Excitation energies ΔE_L (in GeV) of hyperons and mesons for small L in the ρ modes calculated for the Liu-Wong potential model.

S_{12}	0		1	
L \ Hadron	Λ	Mesons	Σ	Mesons
1	0.63	0.83	0.36	0.47
2	0.97	1.32	0.78	0.84
3	1.31	1.65	1.09	1.16

TABLE V. Calculated excitation energies ΔE_L (in GeV) in the ρ mode of hadronic excitations.

	$L=1$	2	3	4	$n=2$
Λ	0.63	0.97	1.31	1.60	0.83
Λ_c	0.65	0.99	1.34	1.65	0.85
Λ_b	0.66	1.01	1.35	1.66	0.73
Σ	0.36	0.78	1.09	1.39	0.71
Σ_c	0.36	0.80	1.12	1.42	0.73
Σ_b	0.36	0.80	1.13	1.44	0.86

TABLE VI. Comparison of the rotational and radial excitations (in GeV) in the λ mode for $\Lambda_i(\Sigma_i)$ families of baryons with the corresponding excitations in the $K,D,b\bar{q}$ ($K^*,D^*,b\,\bar{q}^*$) families of mesons. ω_m is the characteristic excitation energy for the meson.

Baryons	Λ	Λ_c	Λ_b
μ_3	0.140	0.207	0.229
ω_3	0.376	0.339	0.328
ω_m	0.439	0.418	0.411
ΔE_L: $L=1$	0.39	0.34	(0.33)
2	0.70	0.62	(0.61)
3	0.97	0.86	(0.83)
4	1.20	1.07	(1.04)
$n=2$	0.62	0.55	(0.54)
	Σ	Σ_c	Σ_b
ΔE_L: $L=1$	0.35	0.32	(0.31)
2	0.67	0.58	(0.56)
3	0.93	0.82	(0.80)
4	1.17	1.03	(1.00)
$n=2$	0.61	0.53	(0.51)
Mesons	K	D	$b\bar{q}$
$S=0$: $L=1$	0.73	0.56	0.50
2	1.14	0.91	0.85
$n=2$	0.92	0.75	0.71
	K^*	D^*	$b\bar{q}^*$
$S=1$: $L=1$	0.45	0.47	0.47
2	0.81	0.81	0.81
$n=2$	0.70	0.69	0.69

and $\Delta E_L = 0.45$ (0.81) GeV for spin-triplet states. Thus at low orbital excitations in the λ mode, the excitation energies are roughly 85% (60%) of the spin-triplet (spin-singlet) mesonic values. The results of Table VI do not depend substantially on the diquark spin S_{12}, i.e., the quark-diquark spin-spin interaction does not have significant effect on excitation energies. This is presumably because after folding in the diquark size, this effective interaction has become long-ranged. The resulting excitation energies are thus much closer to spin-triplet mesonic values in which spin effects are smaller.

A comparison with Table IV shows that these λ excitation energies are significantly lower than those for ρ excitations. Both modes of excitation are compared with observed spectra for these Λ and Σ states in Figs. 1 and 2. We use the symbols 2, 4, and n to denote the spin doublet, spin quartet, and radial excitations in the λ mode. The corresponding symbols for the ρ mode are D, Q, and R, respectively. The experimental masses are denoted by a horizontal bar or rectangle. An additional question mark denotes a possible structure of only one- or two-star quality in the Particle Data Group table.[17] The orbital angular momentum is also shown for groups for which its value is not obvious.

We see that the observed rotational structure is quite well reproduced. In particular, the $\frac{7}{2}^-(L_\lambda=3)$ state and the $\frac{3}{2}^-$ $(L_\rho=3)$ state in Λ^* are both reproduced, confirming the theoretical expectation that the ρ excitations move rapidly above the λ excitations of the same L as L increases. However, the possible structures of $J^P=\frac{9}{2}^-$ at 1.8 GeV and $\frac{7}{2}^+$ at 2.0 GeV are not accounted for in our model.

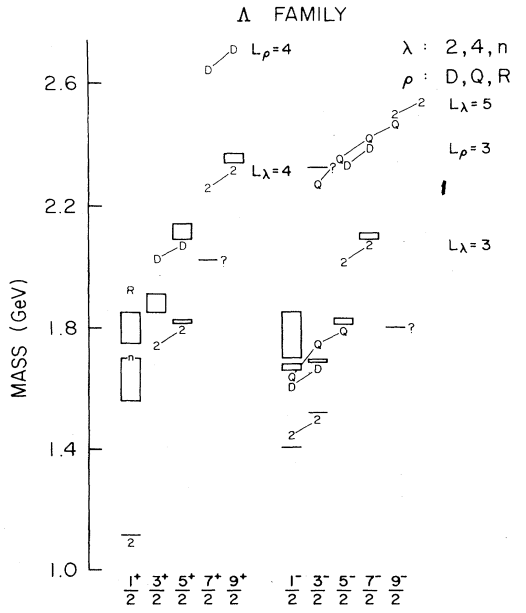

FIG. 1. Comparison of theoretical masses calculated in a single-channel cluster model with experimental masses for the Λ family of baryons. 2,4 (D,Q) denote the spin multiplets in the λ (ρ) mode. n(R) denotes the radial excitation in the λ (ρ) mode. Horizontal lines and rectangles give the experimental masses.

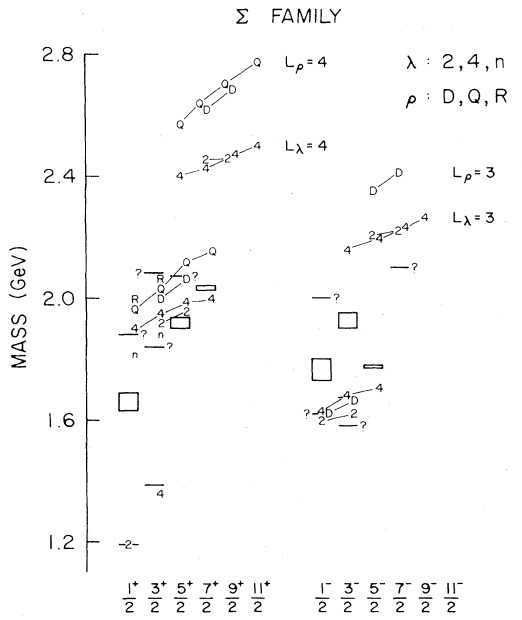

FIG. 2. Comparison of theoretical masses calculated in a single-channel cluster model with experimental masses for the Σ family baryons.

In Σ^* states, the L_ρ and L_λ modes are expected to lie much closer together, although the L_ρ states remain higher. Figure 2 shows good agreement for $L \leq 2$. However, there are three or four broad, questionable, negative-parity structures which appear roughly between the $L=1$ and $L=3$ groups of excited states. It is not clear whether they belong to one group or the other or to none.

For the positive-parity states, the ρ and λ excitations are dynamically mixed. This mixture is carried out via perturbation which will be described in Sec. VI. However, due to the presence of the s quark, the degeneracies between the ρ and λ modes are lifted so that the mixture is much smaller than those in N^* and Δ^*. We shall therefore denote these positive-parity states by their major components. In both Λ^* and Σ^*, the lowest calculated states of radial excitations are those in the λ mode. They are higher than observed masses of the first excited $\frac{1}{2}^+$ states by about 0.1—0.2 GeV. The first radial excitations in the ρ mode lie higher by about 0.2 GeV. This radial excitation in Λ^* should probably be compared with the observed second excited Λ^* state at 1.8 GeV. If so, the model mass is also too high by 0.1—0.2 GeV, but the model ρ-λ mass splitting agrees with the observed value.

Similar analyses can be made of similar excitations in hadrons containing one heavy quark. For excitations in the λ mode we must examine the reduced-mass effect of Eq. (7) carefully because quark masses vary greatly. We find however that their effect is compensated by changes in the fitted strength of the linear confinement potential. Their combined influence on the excitation energy scale ω_3 is quite modest. According to Table VI, it decreases only slightly as we go to heavier quarks. The corresponding excitation energy scale ω_m for mesons is also given in the table, where we find ω_3/ω_m decreasing slightly to 80% (or $2^{-1/3}$) for massive quarks. A more detailed discussion of

the excitations of these heavy hadrons does not appear worthwhile in the absence of experimental masses.

Finally we should mention that in the Ξ families, the diquark is made up of strange quarks while the third quark is the lighter u or d quark. As a result, the ρ excitations appear at lower masses than the corresponding λ excitations. Otherwise the dynamics is describable in the same simple terms, with quite distinct ρ and λ rotational excitations. The calculated results shown in Fig. 3 are of some interest because a number of possible Ξ^* resonances might have been seen,[17] but most of these cannot be plotted in the figure because their spins have not been determined.

V. P-WAVE BARYONS

For baryons with three identical quarks (such as N, Δ, or Ω families), the ρ and λ excitations are degenerate. This is because the Hamiltonian commutes with the permutation operators.[18] This degeneracy is closely, but not exactly, reproduced in our cluster model because of the dissimilar treatments of the ρ and λ degrees of freedom.

For P-wave baryons, there is no dynamical mixing of the ρ and λ modes of excitation, because their orbital wave functions are orthogonal. However, for baryons with three identical quarks, antisymmetrization requires that the wave function contains 50% ρ excitation and 50% λ excitation. This result is readily seen in the usual SU(6)×O(3) classification of states.[19] Thus we take simple averages of calculated masses for appropriate pairs of ρ and λ excited states to generate the correct masses. The results are compared with experimental masses in Table VII. The state labels in the first column give the flavor and spin dimensions.

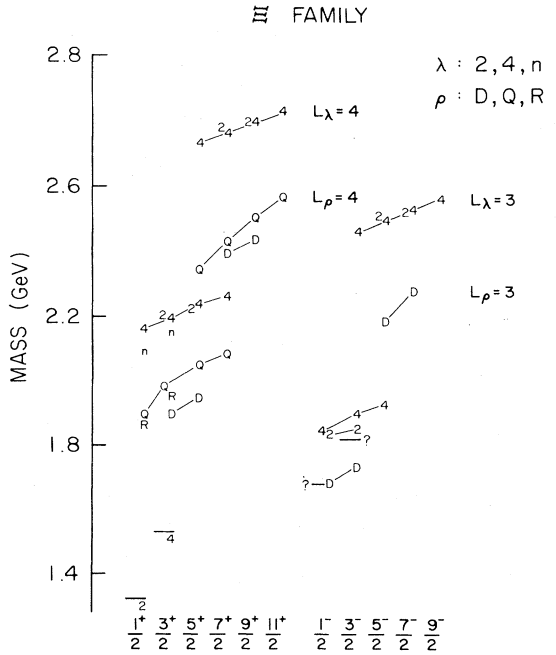

FIG. 3. Comparison of theoretical masses calculated in a single-channel cluster model with experimental masses for the Ξ family of baryons.

TABLE VII. Masses (in MeV) of P-wave N^* and Δ^* baryons. The state labels in the first column give the flavor and spin dimensions. A, original model; B, with zero-range spin-spin interaction; C, no spin-orbit interaction.

State	Calculated A	Calculated B	Calculated C	Experimental
$N^*(8,2)$	1394	1490	~1530	$S11(1520-1560)$
	1453	1540		$D13(1510-1680)$
$N^*(8,4)$	1468	1468		$S11(1620-1680)$
	1592	1592	~1610	$D13(1670-1730)$
	1645	1645		$D15(1660-1690)$
$\Delta^*(10,2)$	1441	1620	~1660	$S31(1600-1650)$
	1489	1670		$D33(1630-1740)$

We see from Table VII that the calculated P-wave N^* and Δ^* masses are lower than the experimental values, except for $D15(1670)$ for which there is agreement. We believe that this can be attributed mostly to the fact that the range of the spin-spin interaction in our $q\bar{q}$ meson potential is too long, thus giving rise to too large hyperfine splittings in the relative P wave. To correct for this, we may impose the additional condition that this spin-spin interaction be switched off when $S_{\text{tot}} < S_{12} + S_3$. If this is done, $S11$ and $D13$ in $N^*(8,2)$ move up by about 90 MeV, while $S31$ and $D33$ move up by about 180 MeV, both in much better agreement with observed masses. If we further switch off the spin-orbit interaction, we will restore the observed near degeneracy of the $N^*(8,4)$ states at $\cong 1610$ MeV. Among these states, $S11(1700)$ and $D13(1700)$ should be further pushed up somewhat by mixing with their $N^*(8,2)$ counterparts through the tensor interaction. This effect has not been included here.

As is well known,[2-5] the observed near degeneracy of the $N^*(8,4)$ states shows that the spin-orbit interaction used to fit the fine splittings in the ρ,ω family is too large for the P-wave baryons. This problem has been discussed by Dalitz,[2] Gromes and Stamatescu,[3] and by Isgur and Karl.[4,5] Recently, Fiebig and Schwesinger[20] have suggested that the needed suppression of the spin-orbit potential might arise from the effects of gluon confinement and of Thomas precession when the problem is treated in the relativistic MIT (Massachusetts Institute of Technology) bag model. Finally, we should point out that the need to have a strong spin-orbit term for light mesons is not as well established as that in charmonium. On the other hand, it is not known experimentally whether the strong spin-orbit potential in charmonium is suppressed in charmed baryons. It thus appears that further theoretical and experimental studies of this spin-orbit problem might be required.

P-wave Λ^* and Σ^* baryons are simpler in structure because λ and ρ excitations appear in different states. Table VIII shows that most calculated masses agree quite well with experimental masses. The agreement would be improved if the spin-spin potential has a shorter range and if the spin-orbit potential is turned off, in agreement with the findings for the N^* and Δ^* states.

TABLE VIII. Masses (in MeV) of P-wave Λ and Σ baryons.

	$2S+1$	J^P	Mode	Calculated	Experiment
Λ^*	2	$\frac{1}{2}^-$	λ	1447	$S01(1405)$
		$\frac{3}{2}^-$	λ	1493	$D03(1519)$
	2	$\frac{1}{2}^-$	ρ	1612	$S01(1660-1680)$
		$\frac{3}{2}^-$	ρ	1672	$D03(1685-1695)$
	4	$\frac{1}{2}^-$	ρ	1631	$S01(1720-1850)$
		$\frac{3}{2}^-$	ρ	1746	
		$\frac{5}{2}^-$	ρ	1789	$D05(1810-1830)$
Σ^*	2	$\frac{1}{2}^-$	ρ	1621	$S11(1620?)$
		$\frac{3}{2}^-$	ρ	1666	$D13(1670?)$
	2	$\frac{1}{2}^-$	λ	1603	$S11(1730-1800)$
		$\frac{3}{2}^-$	λ	1617	$D13(1665-1685)$
	4	$\frac{1}{2}^-$	λ	1618	$S11(1730-1800)$[a]
		$\frac{3}{2}^-$	λ	1677	$D13(1665-1685)$[a]
		$\frac{5}{2}^-$	λ	1705	$D15(1770-1780)$

[a]Alternative assignments.

VI. POSITIVE-PARITY BARYONIC EXCITATIONS

In the SU(6)×O(3) classification, the flavor-spin and the orbital angular momentum contents (flavor-spin multiplet, L^π) for the low-lying excited baryons with positive parities include the following:

$$
\begin{aligned}
&(56',0^+)=S_S=\frac{1}{\sqrt{2}}(\psi_0^\rho+\psi_0^\lambda)\ ,\\
&(70,0^+)=S_M=\begin{cases}\dfrac{1}{\sqrt{2}}(\psi_0^\rho-\psi_0^\lambda)\ ,\\ \psi_0^{\rho\lambda}\ ,\end{cases}\\
&(56,2^+)=D_S=\frac{1}{\sqrt{2}}(\psi_2^\rho+\psi_2^\lambda)\ ,\\
&(70,2^+)=D_M=\begin{cases}\dfrac{1}{\sqrt{2}}(\psi_2^\rho-\psi_2^\lambda)\ ,\\ \psi_2^{\rho\lambda}\ ,\end{cases}\\
&(20,1^+)=P_A=\psi_1^{\rho\lambda}\ ,
\end{aligned}
\tag{10}
$$

where S, P, and D designate the total orbital angular momenta, the subscripts S, M, and A stand for the symmetric, the mixed symmetric, and the antisymmetric permutations of the spatial wave functions. The subscripts of ψ denote the orbital angular momentum L. Unlike P-wave baryons, ψ_L^ρ and ψ_L^λ mix dynamically, so that the degeneracies between $(56',0^+)$ and $(70,0^+)$, and between $(56,2^+)$ and $(70,2^+)$, are removed. The splittings among all these states have been studied in the past. In particular, it has been shown[3,6,21] that the first-order perturbation of any central nonharmonic potential causes various states to move away from their degenerate $N=2$ harmonic oscillator energy by the same relative proportions.

We face a slightly different situation in our cluster model. The splitting between the 0^+ and 2^+ states due to the confinement and color-Coulombic potentials are already included, but different 0^+, or 2^+, states are still degenerate. The unknown splittings can be estimated immediately by using the first-order perturbative pattern of Isgur and Karl[6] mentioned above. For example, the average splitting of our unmixed $\psi_0^\rho/\psi_0^\lambda$ and $\psi_2^\rho/\psi_2^\lambda$ states is about 150 MeV. Since this is 0.45Δ in the Isgur-Karl notation, where Δ is four times the off-diagonal matrix element

$$\langle\psi_0^\rho\,|\,V(\text{confinement}+\text{color Coulombic})\,|\,\psi_0^\lambda\rangle\ ,$$

we immediately have $\Delta\cong 330$ MeV. The Isgur-Karl splittings are then

$$
\begin{aligned}
&\Delta E_0=E(70,0^+)-E(56',0^+)=0.5\Delta\cong 165\ \text{MeV}\ ,\\
&\Delta E_2=E(70,2^+)-E(56,2^+)=0.2\Delta\cong 65\ \text{MeV}\ .
\end{aligned}
\tag{11}
$$

In addition, they also give

$$E(20,1^+)=E(70,2^+)+0.2\Delta\ . \tag{12}$$

As a further check on this procedure, we calculate Δ directly using harmonic-oscillator wave functions. The result is 335 MeV in good agreement with the above result.

Table IX gives our calculated masses including the Isgur-Karl perturbations for the positive parity N^* and Δ^* resonances. They are seen to compare well with the experimental masses. There are several problems, however. The calculated mass of the Roper resonance $P11(1470)$ is still about 150 MeV too high. (We are not free to change the value of Δ to fit its mass, but the effect of tensor mixing of D-wave states has not been included.) The calculat-

TABLE IX. Masses (in MeV) of excited positive-parity N^* and Δ^* baryons labeled by the dominant component as defined in Eq. (10).

	$2S+1$	J^P	Mode	Calculated	Experiment
N^*	2	$\frac{1}{2}^+$	S_S	1620	$P11(1400-1480)$
			S_M	1790	$P11(1680-1740)$
	4	$\frac{1}{2}^+$	D_M	1800	
	2	$\frac{3}{2}^+$	D_S	1732	$P13(1690-1800)$
		$\frac{3}{2}^+$	D_M	1800	
	4	$\frac{3}{2}^+$	D_M	1878	
		$\frac{3}{2}^+$	S_M	1944	
	2	$\frac{5}{2}^+$	D_S	1802	$F15(1670-1690)$
			D_M	1870	
	4	$\frac{5}{2}^+$	D_M	1971	$F15(2000?)$
		$\frac{7}{2}^+$	D_M	2028	$F17(1950-2050)$
Δ^*	2	$\frac{1}{2}^+$	S_M	1810	$P31(1850-1950)$
	4	$\frac{1}{2}^+$	D_S	1733	
		$\frac{3}{2}^+$	S_S	1777	$P33(1500-1900)$
		$\frac{3}{2}^+$	D_S	1810	
	2	$\frac{3}{2}^+$	D_M	1821	$P33(1860-2160)$
		$\frac{5}{2}^+$	D_M	1903	$F35(1890-1920)$
	4	$\frac{5}{2}^+$	D_S	1877	
		$\frac{7}{2}^+$	D_S	1960	$F37(1910-1960)$

ed mass for $\Delta^*(\frac{1}{2}^+, D_S)$ at 1733 MeV is lower than the experimental value for $P31(1910)$. This suggests again that the spin-orbit interaction is far too strong.

For the Λ^* and Σ^* states, the presence of an s quark means that the unmixed λ and ρ modes are no longer degenerate because (primarily) of the reduced-mass effect. There is an additional dynamical mixing, which is handled as follows. The off-diagonal matrix element $\Delta/4$ is estimated from the spacing between the mean positions of $\psi_0^\rho/\psi_0^\lambda$ and $\psi_2^\rho/\psi_2^\lambda$ to be 59 MeV for Λ^* and 71 MeV for Σ^*. A 2×2 matrix is then diagonalized for each set of L states to give the final results. Table X shows that these calculated values compare quite favorably with the experimental masses.

We should mention that we have not calculated the masses of the $\psi_0^{\rho\lambda}$, $\psi_2^{\rho\lambda}$, and $\psi_1^{\rho\lambda}$ (P_A) states, but they are all calculable in our cluster model if we use a P-wave variational function for one of the internal coordinates.

We have done similar calculations for the baryon families Ξ, Ω, Λ_c, Σ_c, Λ_b, and Σ_b. In Table XI, we report on the calculated results for only the lowest-mass state of each J^P. These states have not been observed experimentally.

VII. CONCLUSIONS

We have shown that it is possible to use a cluster approach to study excited states in baryons and that this approach is also useful because it emphasizes the similarities and differences in quark dynamics as manifested in baryon masses as compared to meson masses. We have further shown that the use of only two-body quark-quark potentials deduced from meson spectra can give a rough picture of baryon masses even in such an unsophisticated model as a nonrelativistic potential model. Finally, we want to mention once more some of the limitations of our oversimplified model—the unrealistic description of kinetic energies, the need to lower all baryon masses by about 100 MeV, and the need to suppress the strong spin-orbit potential at least in certain states.

ACKNOWLEDGMENT

This work is supported in part by NSF Contract No. PHY78-15811 and DOE Contract DE-AS05-82ER40074.

APPENDIX

Equation (8) is the cluster Hamiltonian for the ρ mode with the contribution from the third particle folded into the variational wave function in the S wave

$$\phi_\lambda = \left[\frac{2\alpha}{\pi}\right]^{3/4} e^{-\alpha\lambda^2} . \tag{A1}$$

The kinetic-energy contribution due to the third particle is therefore

TABLE X. Masses (in MeV) of excited positive-parity Λ^* and Σ^* baryons labeled by the dominant mode of orbital excitation.

	$2S+1$	J^P	Mode	Calculated	Experiment
Λ^*	2	$\frac{1}{2}^+$	S_λ	1693	$P01(1560-1700)$
			S_ρ	1930	$P01(1750-1850)$
	2	$\frac{3}{2}^+$	D_λ	1744	$P03(1850-1910)$
			D_ρ	2034	
	2	$\frac{5}{2}^+$	D_λ	1795	$F05(1815-1825)$
			D_ρ	2087	$F05(2090-2140)$
Σ^*	2	$\frac{1}{2}^+$	S_λ	1820	$P11(1630-1690)$
	4	$\frac{1}{2}^+$	D_λ	1896	$P11(1880?)$
	2	$\frac{1}{2}^+$	S_ρ	1994	
	4	$\frac{1}{2}^+$	D_ρ	1969	
	4	$\frac{3}{2}^+$	S_λ	1884	$P13(1840?)$
			S_ρ	2065	$P13(2080?)$
	2	$\frac{3}{2}^+$	D_λ	1927	
			D_ρ	2001	
	4	$\frac{3}{2}^+$	D_λ	1934	
			D_ρ	2033	
	2	$\frac{5}{2}^+$	D_λ	1948	$F15(1900-1935)$
			D_ρ	2064	$F15(2070?)$
	4	$\frac{5}{2}^+$	D_λ	1977	
			D_ρ	2115	
	4	$\frac{7}{2}^+$	D_λ	2004	$F17(2025-2040)$
			D_ρ	2161	

$$\langle P_\lambda^2/2\mu_3\rangle_{L=0}=\frac{3\alpha}{2\mu_3} ,$$

where

$$\mu_3=\frac{(m_1+m_2)m_3}{m_1+m_2+m_3} . \tag{A2}$$

The convolution operator C for the potential contribution is defined as

$$C[V_{13}](\rho/2)=\left[\frac{2\alpha}{\pi}\right]^{3/2}\int d^3r_{13}e^{-2\alpha(\vec{\rho}/2-\vec{r}_{13})^2}V(r_{13}) . \tag{A3}$$

TABLE XI. Calculated masses (in MeV) of the lowest-mass states of each J^P for a number of baryon families. The spin-orbit and the tensor interactions are neglected in Λ_c^*, Σ_c^*, Λ_b^*, and Σ_b^*.

J^P	$\frac{1}{2}^+$	$\frac{3}{2}^+$	$\frac{5}{2}^+$	$\frac{7}{2}^+$
Ξ^*	1850	1954	1950	2084
Ω^*	2168	2105	2210	2237
Λ_c^*	2763	2836	2836	
Σ_c^*	2957	2957	3017	3017
Λ_b^*	6050	6120	6120	
Σ_b^*	6148	6148	6302	6302

For the central and spin-spin potentials

$$V_{13}^{C}=-\tfrac{3}{16}(kr_{13}+b')+\frac{\alpha_s}{4}\frac{1}{r_{13}} ,$$
$$V_{13}^{SS}=\frac{\alpha_s}{16m_1m_3}S(r_{13}) , \tag{A4}$$

the convolution integrals yield for each term the following expressions:

$$C[1/r_{13}](\rho/2)=\frac{2}{\rho}\,\mathrm{erf}(\sqrt{2\alpha}\rho/2) ,$$

$$C[r_{13}](\rho/2)=\frac{1}{\sqrt{2\pi\alpha}}e^{-2\alpha(\rho/2)^2}+\frac{\rho}{2}\,\mathrm{erf}(\sqrt{2\alpha}\rho/2)$$
$$+\frac{1}{2\alpha\rho}\,\mathrm{erf}(\sqrt{2\alpha}\rho/2) , \tag{A5}$$

$$C[S](\rho/2)=S(0)\exp\left\{-\left[\frac{2\alpha/r_0}{2\alpha+1/r_0^2}(\rho/2)^2\right]\right\}$$
$$\times\left[\frac{2\alpha}{2\alpha+1/r_0^2}\right]^{3/2} .$$

For the spin-orbit potential

$$V_{13}^{\mathrm{SO}}=\frac{\alpha_s}{4m_1m_3}W(r_{13}) \ , \tag{A6}$$

the convolution gives

$$C[\vec{\mathrm{L}}_{13}W(r_{13})]=\left\{\tfrac{1}{2}C[W](\rho/2)+\frac{1}{4\alpha\rho}\frac{d}{d(\rho/2)}C[W](\rho/2)\right\}\vec{\mathrm{L}}_{12} \ . \tag{A7}$$

To evaluate $C[W](\rho/2)$ at short distance, we expand W as

$$W(r_{13})=-\frac{3}{2}\frac{1}{{r_{13}}^3}(1-e^{-\beta {r_{13}}^2})=\sum_{n=1}^{\infty}C_n{r_{13}}^{2n-2} \ , \tag{A8}$$

where

$$C_n=-\tfrac{3}{2}(-)^{n+1}\beta^n/n!, \quad \beta=1/{a_0}^2 \ .$$

Hence

$$C[W](\rho/2)=\sum_{n=1}^{\infty}C_nW_{2n}(\rho/2)=\sum_{n=1}^{\infty}C_n\left[-\frac{\partial}{\partial\gamma}\right]^{n-1}W_2(\rho/2,\gamma)\,|_{\gamma=2\alpha} \ , \tag{A9}$$

with

$$W_2(\rho/2,\gamma)=-\frac{3}{2}\left[\frac{2\alpha}{\gamma}\right]^{1/2}e^{-2(2\alpha^2/\gamma-\alpha)(\rho/2)^2}\,\mathrm{erf}\left[\frac{\alpha\rho}{\sqrt{\gamma}}\right]\Big/(\rho/2) \ . \tag{A10}$$

We find more specifically that

$$W_2(\rho/2)=-\tfrac{3}{2}\,\mathrm{erf}(\sqrt{2\alpha}\rho/2)/(\rho/2) \ ,$$

$$W_4(\rho/2)=-\frac{3}{2}\left\{\left[\frac{1}{4\alpha}+(\rho/2)^2\right]\mathrm{erf}(\sqrt{2\alpha}\rho/2)+\frac{\rho/2}{\sqrt{2\alpha\pi}}e^{-2\alpha(\rho/2)^2}\right\}\Big/(\rho/2) \ , \tag{A11}$$

$$W_6(\rho/2)=-\frac{3}{2}\left\{\left[\frac{3}{16\alpha^2}+\frac{3(\rho/2)^2}{2\alpha}+(\rho/2)^4\right]\mathrm{erf}(\sqrt{2\alpha}\rho/2)+\left[\frac{5}{4\alpha}+(\rho/2)^2\right]\frac{\rho/2}{\sqrt{2\pi\alpha}}e^{-2\alpha(\rho/2)^2}\right\}\Big/(\rho/2), \text{ etc.}$$

Asymptotically, $C[W](\rho/2)$ approaches $W(\rho/2)$. This is implemented by matching the truncated series of Eq. (A9) to $W(\rho/2)$ using the following approximation:

$$C[W](\rho/2)\to\left[\sum_{n=1}^{3}C_nW_{2n}(\rho/2)\right]e^{-\delta(\rho/2)^2}+(1-e^{-\delta(\rho/2)^2})W(\rho/2) \ , \tag{A12}$$

where δ is chosen to be $\alpha/3$ so that the match distance is greater than $\langle\lambda^2\rangle^{1/2}$, the rms radius of the third particle from the center of the diquark. Since the tensor potential has the same form as that of $W(r_{13})$, we applied the same procedure to evaluate $C[V^T]$ as was done for $C[W]$.

For the λ mode, the cluster Hamiltonian is written as

$$\begin{aligned}H_\lambda=&m_1+m_2+m_3+\langle {P_\rho}^2/2\mu_{12}\rangle_{L=0}+\lambda_1\cdot\lambda_2\langle V_{12}\rangle_{L=0}+{P_\lambda}^2/2\mu_3\\&+(\lambda_1+\lambda_2)\cdot\lambda_3\{C[V_{13}^{\mathrm{C}}](\lambda)+2\vec{\mathrm{S}}_{12}\cdot\vec{\mathrm{S}}_3C[V_{13}^{\mathrm{SS}}](\lambda)+(\tfrac{1}{2}\vec{\mathrm{S}}_{12}+\vec{\mathrm{S}}_3)\cdot C[\vec{\mathrm{L}}_{13}V_{13}^{\mathrm{SO}}](\lambda)\\&+2(3\vec{\mathrm{S}}_{12}\cdot\hat{\lambda}\,\vec{\mathrm{S}}_3\cdot\hat{\lambda}-\vec{\mathrm{S}}_{12}\cdot\vec{\mathrm{S}}_3)C[V_{13}^{T}](\lambda)\} \ .\end{aligned} \tag{A13}$$

In this case, the contributions from the diquark pair are folded in by using the variational wave function

$$\phi_\rho=\left[\frac{2\alpha}{\pi}\right]^{3/4}e^{-\alpha\rho^2} \ . \tag{A14}$$

We obtain

$$\langle {P_\rho}^2/2\mu_{12}\rangle_{L=0}=\frac{3\alpha}{2\mu_{12}} \ ,$$

and

$$\langle V_{12}\rangle_{L=0}=-\frac{3}{16}\left[\frac{k}{\sqrt{2\pi\alpha}}+b'\right]+\frac{\alpha_s\alpha}{\sqrt{2\pi}}-\frac{\alpha_s}{6\sqrt{\pi}m_1m_2}\frac{1}{r_0{}^3}\left[\frac{2\alpha}{2\alpha+1/r_0{}^2}\right]^{3/2}\vec{\sigma}_1\cdot\vec{\sigma}_2 \ . \tag{A15}$$

The convolution operation defined as

$$C[V_{13}](\lambda)=\left[\frac{2\alpha}{\pi}\right]^{3/2}\int d^3r_{13}e^{-2\alpha(\vec{\lambda}-\vec{r}_{13})^2}V(r_{13}) \tag{A16}$$

is the same as $C[V_{13}](\rho/2)$ when the argument $\rho/2$ is replaced by λ.

[1]J. J. J. Kokkedee, *The Quark Model* (Benjamin, New York, 1969).
[2]R. H. Dalitz, Prog. Part. Nucl. Phys. 8, 7 (1982).
[3]D. Gromes and I. O. Stamatescu, Nucl. Phys. B112, 213 (1976).
[4]N. Isgur and G. Karl, Phys. Lett. 72B, 109 (1977).
[5]N. Isgur and G. Karl, Phys. Rev. D 18, 4187 (1978).
[6]N. Isgur and G. Karl, Phys. Rev. D 19, 2653 (1979).
[7]N. Isgur and G. Karl, Phys. Rev. D 20, 1191 (1979).
[8]C. W. Wong, Prog. Part. Nucl. Phys. 8, 223 (1982).
[9]I. Cohen and H. J. Lipkin, Phys. Lett. 93B, 56 (1980).
[10]A. De Rújula, H. Georgi, and S. L. Glashow, Phys. Rev. D 12, 147 (1975).
[11]K. F. Liu and C. W. Wong, Phys. Rev. D 17, 2350 (1978).
[12]J. F. Rondinone, Ph.D. thesis, UCLA, 1978 (unpublished).
[13]D. P. Stanley and D. Robson, Phys. Rev. Lett. 45, 235 (1980).
[14]K. F. Liu and C. W. Wong, Phys. Lett. 107B, 391 (1981).
[15]K. F. Liu and C. W. Wong, Phys. Rev. D 21, 1350 (1980).
[16]D. B. Lichtenberg and R. L. Johnson, Hadronic J. 2, 1 (1979); D. B. Lichtenberg, Phys. Rev. D 22, 1225 (1980); D. B. Lichtenberg, W. Namgung, E. Predazzi, and J. G. Wills, Phys. Rev. Lett. 48, 1653 (1982); D. B. Lichtenberg, W. Namgung, J. G. Wills, and E. Predazzi, Indiana University report, 1982 (unpublished).
[17]Particle Data Group, Phys. Lett. 111B, 1 (1982).
[18]M. Harvey, private communication.
[19]F. E. Close, *An Introduction to Quarks and Partons* (Academic, London, 1979), pp. 80–92.
[20]H. R. Fiebig and B. Schwesinger, Nucl. Phys. A393, 349 (1983).
[21]R. Horgan and R. H. Dalitz, Nucl. Phys. B66, 135 (1973).